

Supplementary Materials: Regional Scale Rain-Forest Height Mapping Using Regression-Kriging of Spaceborne and Airborne LiDAR Data: Application on French Guiana. *Remote Sensing* 2016, 8, manuscript ID

Ibrahim Fayad, Nicolas Baghdadi, Jean-Stéphane Bailly, Nicolas Barbier, Valéry Gond, Bruno Hérault, Mahmoud El Hajj, Frédéric Fabre and José Perrin

Table S1. Non-exhaustive summary of studies using radar data to estimate canopy heights with PolInSAR (polarimetric interferometric SAR) and tomography techniques.

| Technique | Accuracy | Limitations | References |
|--|---|---|------------|
| PolInSAR (Spaceborne data) | Errors of 8 and 12.8 m were observed for residual relative and absolute height respectively | Data affected by high sources of errors. | [1] |
| P-band PolInSAR (Airborne) | 2 m RMSE on the canopy height estimates for 2 to 25 m tall stands | Viable for small areas. | [2] |
| L-band PolInSAR (Airborne) | 3 m RMSE 2 m RMSE on the canopy height estimates for 35 m stands | Viable for small areas. Saturation at higher stand heights | [3] |
| P-band SAR tomography (Airborne) | 7.7 m RMSE on the canopy height estimation | Low estimation accuracy | [4] |
| L-band SAR tomography (Airborne) | 10% relative error on canopy height estimates in comparison to LiDAR esimtaes | Viable for small areas. Low estimation accuracy | [5] |

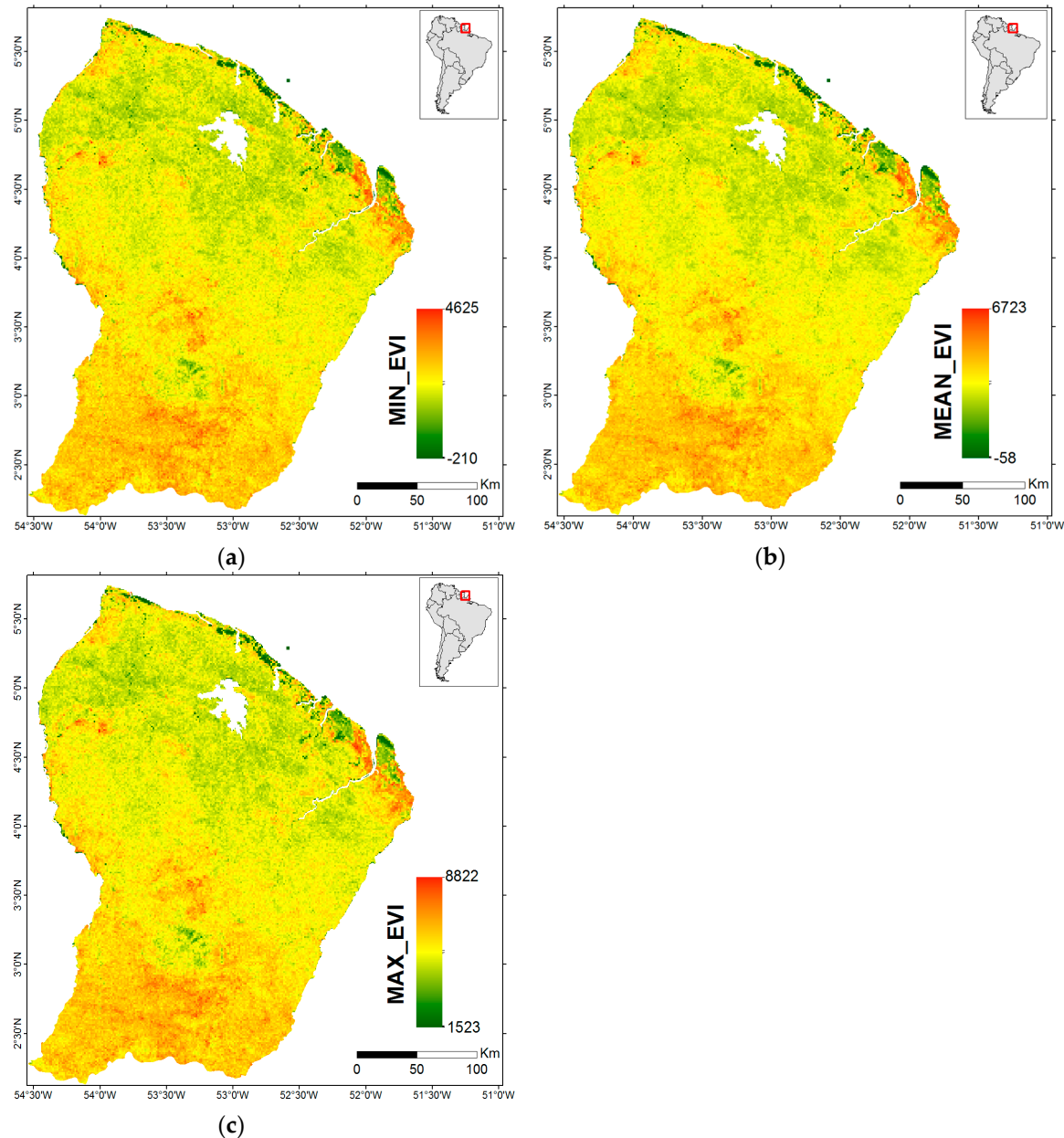


Figure S1. Minimum (a); mean (b); and maximum (c) values of the EVI time series data.

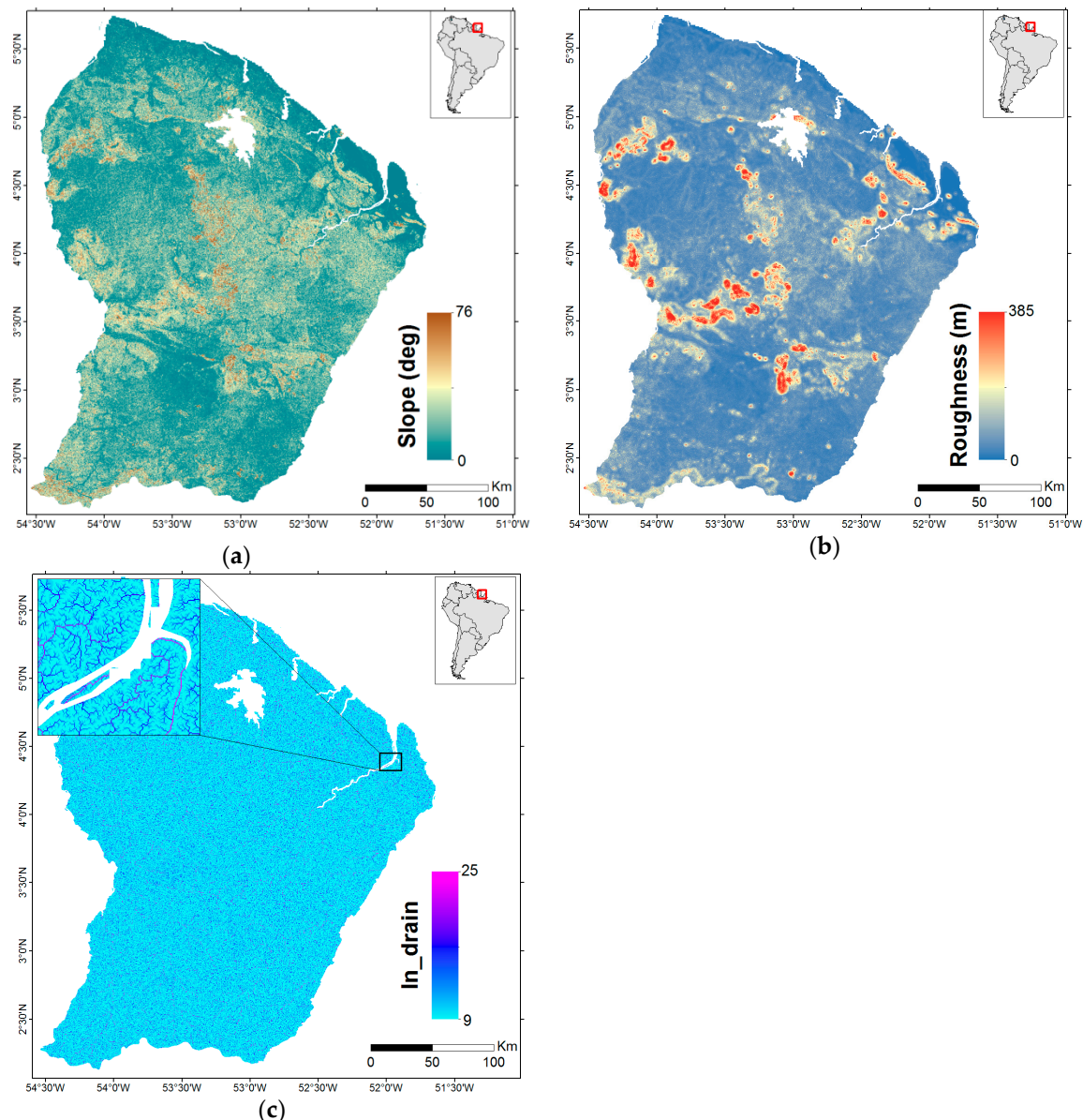


Figure S2. SRTM DEM derived maps: slope map “in degrees” (a); surface roughness map “in m” (b); and drainage surface map (c).

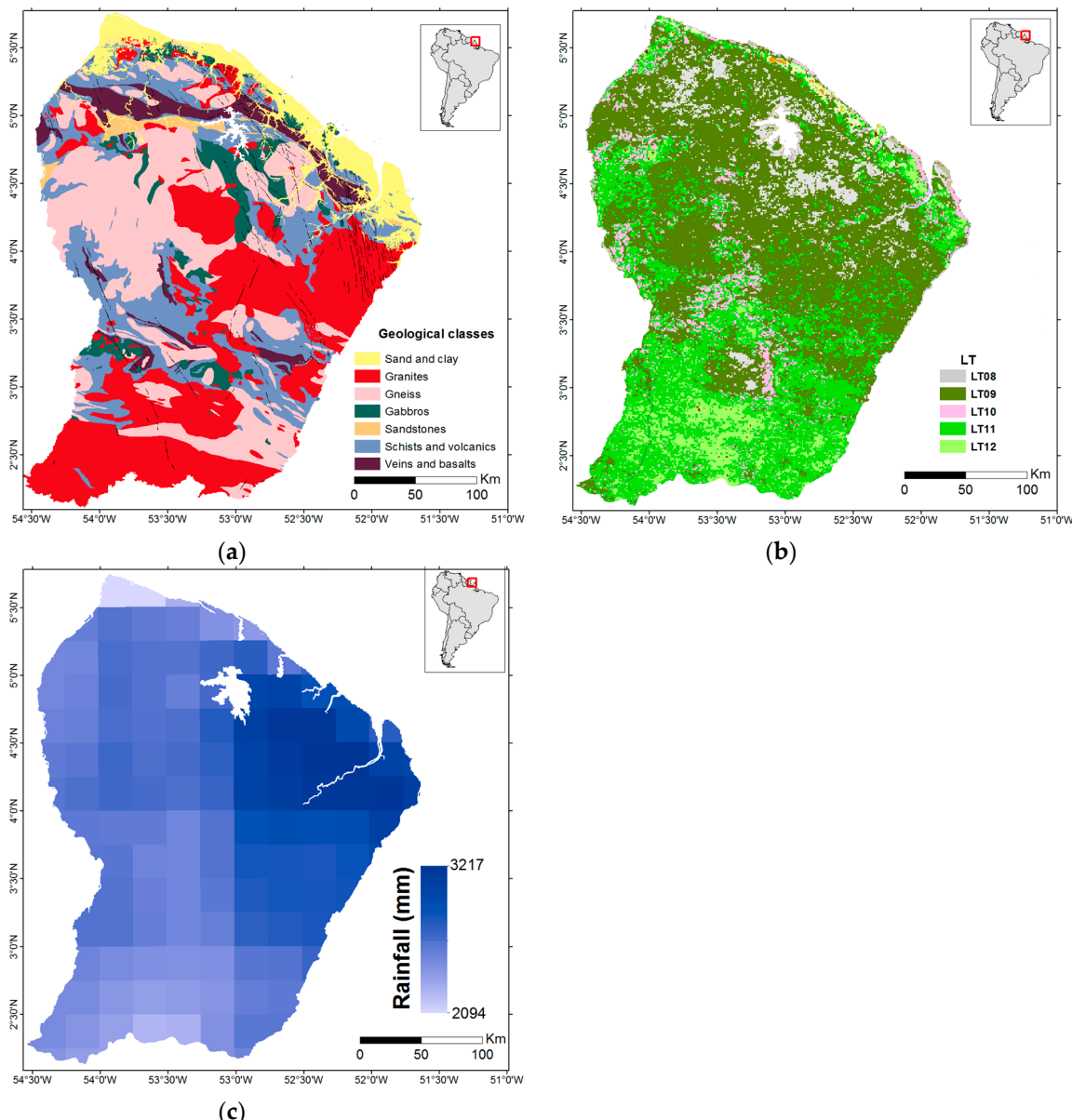


Figure S3. Geological map (a); Forest landscape types map (b); and Average rainfall map (c).

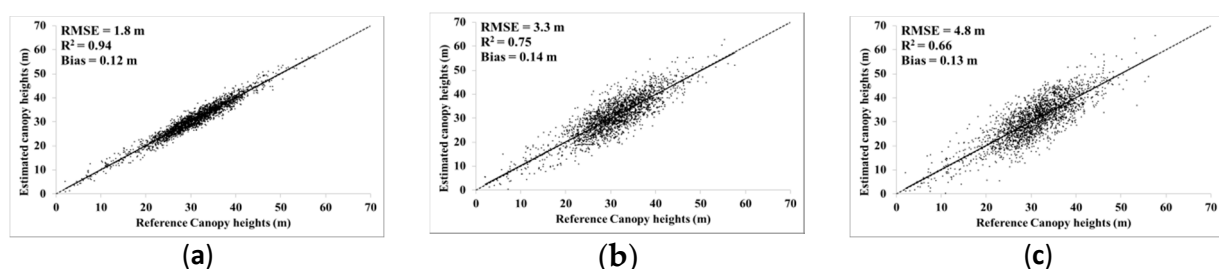


Figure S4. Comparison between reference canopy heights of the validation datasets (LD_val and HD) and canopy height estimates using Random Forest regressions and residual-kriging for (a) LD_5; (b) LD_20; (c) LD_50.

References

1. Castel, T.; Beaudoin, A.; Trouche, G. Analysis of SAR interferometry for tree height. *Agricultura* **2002**, *1*, 15–23.
2. Garestier, F.; Dubois-Fernandez, P.; Champion, I. Forest Height Inversion Using High-Resolution P-Band Pol-InSAR Data. *IEEE Trans. Geosci. Remote Sens.* **2008**, *46*, 3544–3559.

3. Neumann, M.; Hensley, S.; Lavalle, M.; Ahmed, R. Forest Structure Characterization Using Jpl'S Uavstar Multi-Baseline. In Proceedings of the 4th Asia-Pacific Conference on Synthetic Aperture Radar, Tsukuba, Japan, 23–27 September 2013.
4. Huang, Y.; Ferro-Famil, L.; Reigber, A. Under-Foliage Object Imaging Using SAR Tomography and Polarimetric Spectral Estimators. *IEEE Trans. Geosci. Remote Sens.* **2011**, *50*, 2213–2225.
5. Mercer, B.; Zhang, Q.; Schwaebisch, M.; Denbina, M.; Cloude, S. Forest height and ground topography at L-band from an experimental single-pass airborne PolInSAR system. In Proceedings of the PolInSAR 2009 Workshop, Frascati, Italy, 26–30 January 2009.



© 2016 by the authors; licensee MDPI, Basel, Switzerland. This article is an open access article distributed under the terms and conditions of the Creative Commons by Attribution (CC-BY) license (<http://creativecommons.org/licenses/by/4.0/>).